



# Estimating the teleported initial parameters of a single- and two-qubit systems

K. El Anouz<sup>1</sup> · A. El Allati<sup>1,2</sup> · N. Metwally<sup>3,4</sup> · T. Mourabit<sup>1</sup>

Received: 13 July 2018 / Accepted: 7 December 2018 / Published online: 15 December 2018  
© Springer-Verlag GmbH Germany, part of Springer Nature 2018

## Abstract

A single atomic field state is used as a quantum channel to teleport a state of two-qubit system. The possibility of estimating the teleported initial state parameters is discussed by means of quantum Fisher information. It is shown that by controlling the initial atomic field parameters, one may freeze the quantum Fisher information of the teleported parameters. Meanwhile, the teleported state keeps its local information. The sizes of the frozen areas depend on the initial state settings and the atomic field parameters. We show that the estimation degree of teleporting a single qubit is larger than that depicted for two-qubit system. Moreover, the estimation degree increases in the resonance case. It is shown that the maximum bounds of the quantum Fisher information are reached periodically. The phenomena of the sudden changes of quantum Fisher information are displayed at larger values of detuning parameters and the number of photons inside the cavity.

## 1 Introduction

Quantum teleportation is one of the most fascinating protocols predicted by quantum mechanics [1]. It is a critical ingredient for quantum communication and quantum computation networks [2–4]. Quantum teleportation is a faithful transfer of quantum states between two distant parties which have established prior entanglement and can communicate classically. In the past two decades, quantum teleportation has attracted considerable attentions and been studied both theoretically and experimentally [5–7]. However, in many scenarios, one does not need to teleport the whole quantum state, but rather the information of a particular parameter physically encoded in it. Therefore, there is no need to teleport the full information of the quantum states themselves, but only the relevant parameters that carry these

information. In contrast to the quantum state teleportation where the credibility of teleportation is measured by fidelity, the transmission of information that is carried by a physical parameter is usually quantified by quantum Fisher information (QFI) [8, 9]. QFI plays a significant role in the fields of quantum geometry of state spaces [8, 10, 11], quantum information theory [12] and quantum metrology [13, 14]. Particularly, the inverse of QFI characterizes the ultimate achievable precision in parameter estimation [15]. In other words, QFI is used as an estimation tool of parameters that are contained in a quantum system during its evolution [16]. Due to its importance, there are some efforts that have been taken to quantify QFI in different quantum systems.

Recently, some authors have paid attention to quantifying quantum Fisher information in open quantum systems. For example, Zheng et al. [17] investigated the dynamics of QFI for a two-qubit system, where each qubit interacts with its own Markovian environment. Ozaydin [18] has quantified the QFI analytically for the W-state in the presence of different noisy channels. The effect of the Markovian reservoirs on the dynamics of the quantum Fisher information of a two-level system is discussed by You et al. [19]. Quantum Fisher information for a noisy open quantum system and initially prepared in a steady state is quantified by Altinats [20]. In the context of accelerated system, Metwally [21] discussed the possibility of quantifying the teleported by means of quantum Fisher information. Estimating the weight and the phase parameters

✉ A. El Allati  
abdou.allati@gmail.com

<sup>1</sup> Laboratory of R&D in Engineering Sciences, Faculty of Sciences and Techniques Al-Hoceima, Abdelmalek Essaadi University, Tétouan, Morocco

<sup>2</sup> The Abdus Salam International Center for Theoretical Physics, Strada Costiera 11, Miramare-Trieste, Italy

<sup>3</sup> Mathematics Department, College of Science, University of Bahrain, P. O. Box 32038, Bahrain, Kingdom of Bahrain

<sup>4</sup> Mathematics Department, Faculty of Science, Aswan University, Aswan, Egypt

of pulsed driven qubit via quantum Fisher information, where different pulses are considered [22].

In this context, it is important to mention some applications of quantum Fisher information. However, in the additional of using it as a quantifier of the initial parameters that describe the state, it can be used to calculate the phase sensitivity of systems that provides in quantum technologies, as example it can be used to enhance the imaging process without increasing the illumination power [23]. Since it may be frozen during the evaluation of the quantum system and consequently the information which is encoded in this system, then quantum Fisher information may be used as resource of secure communication [24]. It may be used to process the large amount of data that is needed for quantum computer [25]. Moreover, the quantum Fisher information also quantifies the degree of macroscopicity of a quantum state [26].

In the present work, we use a single atomic-field state, to teleport a two-qubit system. The possibility of estimating the teleported parameters is discussed by the quantum Fisher information of the two-qubit as well as by a single qubit. The effect of the atomic-field parameters on the estimation degree of the teleported parameters are discussed. We show that, it is possible to freeze the quantum Fisher information by controlling the initial state parameters and the atomic-field parameters.

The paper is organized as follows. In Sect. 2, we introduce the suggested model, where an analytical solution in terms of the Bloch vector is given. In Sect. 3, the possibility of teleporting the quantum Fisher information is discussed, where a description of a quantum teleportation protocol of a two-qubit system is reviewed. A mathematical form of the quantum Fisher information is introduced for a single and two-qubit systems. In Sect. 4, the weight and the phase parameters of the teleported state are quantified at the resonance and non-resonance cases, where some numerical calculations are presented. Finally, our results are summarized at Sect. 5.

## 2 Description of the model

The suggested system is described by Jaynes Cummings model of a single-two level atom interacts with a single cavity mode. In the rotating wave approximation, the Hamiltonian of this system is governed by [27, 28]

$$H = \frac{1}{2}\omega_0\sigma_z + \omega a^\dagger a + g(a|e\rangle\langle g| + a^\dagger|g\rangle\langle e|),$$

where, the first two terms represent the Hamiltonian of the atom and the cavity mode, respectively, while the third term

represents the interaction Hamiltonian. The parameters  $\omega_0$  and  $\omega$  are the frequencies of the atomic system and the cavity mode, respectively, and the operators  $a^\dagger$  ( $a$ ) represent the creation (annihilation) operators of the cavity mode,  $|e\rangle$  and  $|g\rangle$  are the excited and the ground states of the atom, respectively, and  $g$  is the constant coupling between the atomic system and the cavity mode.

Let us assume that, the atomic-cavity system is initially prepared in a product state  $|\psi_s(0)\rangle = |\psi_f\rangle \otimes |\psi_a\rangle$

$$|\psi_s(0)\rangle = \sum_{n=0}^{\infty} P_n |n, e\rangle, \tag{1}$$

where  $|\psi_a(0)\rangle = |e\rangle$  and  $|\psi_f(0)\rangle = \sum_0^\infty P_n |n\rangle$ ,  $P_n = \exp(-\frac{\bar{n}}{2}) \sqrt{\frac{\bar{n}^n}{n!}}$  with  $\bar{n}$  is the mean photons number. For any  $t > 0$ , the time evolution of the total system is given by:

$$|\psi_s(t)\rangle = \mathcal{U}(t)|\psi_s(0)\rangle, \tag{2}$$

where  $\mathcal{U}(t)$  is the time evolution operator. In the atomic basis  $|e\rangle$  and  $|g\rangle$ , the operator  $\mathcal{U}(t)$  may be written as,

$$\mathcal{U}(t) = \begin{pmatrix} c(\hat{n} + 1, t) & d(\hat{n} + 1, t)a \\ -a^\dagger d^\dagger(\hat{n} + 1, t) & c^\dagger(\hat{n}, t) \end{pmatrix}, \tag{3}$$

where,

$$\begin{aligned} c(\hat{n}, t) &= e^{i\delta\tau} \left[ \cos(\tau\sqrt{\delta^2 + \hat{n}}) - i\frac{\delta}{\sqrt{\delta^2 + \hat{n}}} \sin(\tau\sqrt{\delta^2 + \hat{n}}) \right], \\ d(\hat{n}, t) &= -i\frac{e^{i\delta\tau}}{\sqrt{\delta^2 + \hat{n}}} \sin(\tau\sqrt{\delta^2 + \hat{n}}), \end{aligned} \tag{4}$$

and  $\hat{n} = a^\dagger a$  is the number operator,  $\tau = gt$  and  $\delta = \Delta/2g$  is the dimensionless detuning. Using (2–4), the time evolution of the atom-field state is given by

$$\begin{aligned} |\psi(t)\rangle &= \sum_{n=0}^{\infty} \left( \cos(\tau\sqrt{\delta^2 + \hat{n}}) - i\frac{\delta}{\sqrt{\delta^2 + \hat{n}}} \sin(\tau\sqrt{\delta^2 + \hat{n}}) |n, e\rangle \right. \\ &\quad \left. - ie^{-i\delta\tau} \frac{\sqrt{n+1}}{\sqrt{\delta^2 + (n+1)}} \sin(\tau\sqrt{\delta^2 + \hat{n}}) |n+1, g\rangle \right). \end{aligned} \tag{5}$$

It is clear that, this state represents the final state of the total system in  $2 \times \infty$ -dimensional space. In this context, we consider the minimum amount of entanglement that generated between the atom and the cavity. So, we have to project this final state in a  $2 \times 2$  dimensional subspace, which could be done by a local action only [29]. In the two-dimensional space, the atomic-field state is collapses to be,

$$\begin{aligned} \rho_{af}(t) &= \rho_{11}|n, g\rangle\langle n, g| + \rho_{22}|n, e\rangle\langle n, e| + \rho_{23}|n, e\rangle\langle n+1, g| + \rho_{23}^*|n+1, g\rangle\langle n, e| \\ &\quad + \rho_{33}|n+1, g\rangle\langle n+1, g| + \rho_{44}|n+1, e\rangle\langle n+1, e|, \end{aligned} \tag{6}$$

where

$$\begin{aligned} \rho_{11} &= \frac{P_{n-1}^2}{\mathcal{N}} \frac{n}{\delta^2 + n} \sin^2 \left( \tau \sqrt{\delta^2 + n} \right), \\ \rho_{22} &= \frac{P_n^2}{\mathcal{N}} \left[ \cos^2 \left( \tau \sqrt{\delta^2 + (n+1)} \right) + \frac{\delta^2}{\delta^2 + (n+1)} \sin^2 \left( \tau \sqrt{\delta^2 + (n+1)} \right) \right], \\ \rho_{23} &= i \frac{P_n^2 \sqrt{n+1} e^{-i\delta\tau}}{\mathcal{N} \sqrt{\delta^2 + (n+1)}} \sin \left( \tau \sqrt{\delta^2 + (n+1)} \right) \left[ \cos \left( \tau \sqrt{\delta^2 + (n+1)} \right) - i \frac{\delta \sin \left( \tau \sqrt{\delta^2 + (n+1)} \right)}{\sqrt{\delta^2 + (n+1)}} \right], \\ \rho_{32} &= \rho_{23}^*, \\ \rho_{33} &= \frac{P_n^2}{\mathcal{N}} \frac{(n+1)}{\delta^2 + (n+1)} \sin^2 \left( \tau \sqrt{\delta^2 + (n+1)} \right), \\ \rho_{44} &= \frac{P_{n+1}^2}{\mathcal{N}} \left[ \cos^2 \left( \tau \sqrt{\delta^2 + (n+1)} \right) + \frac{\delta^2}{\delta^2 + (n+1)} \sin^2 \left( \tau \sqrt{\delta^2 + (n+1)} \right) \right], \end{aligned} \tag{7}$$

and  $\mathcal{N}$  is the normalization factor is given by,

$$\begin{aligned} \mathcal{N} &= P_n^2 + \left[ \frac{n}{\delta^2 + n} \sin^2 \left( \tau \sqrt{\delta^2 + n} \right) \right] P_{n-1}^2 \\ &\quad + \left[ \cos^2 \left( \tau \sqrt{\delta^2 + (n+1)} \right) + \frac{\delta^2}{\delta^2 + (n+1)} \sin^2 \left( \tau \sqrt{\delta^2 + (n+1)} \right) \right] P_{n+1}^2. \end{aligned} \tag{8}$$

### 3 Teleporting quantum Fisher information

In this section, we quantify the amount of the teleported quantum Fisher information that contained in a two-qubit state, by means of quantum teleportation. We investigate the effect of the field and atomic parameters on the behavior of the quantum Fisher information.

#### 3.1 Teleportation protocol

In this context, we use a protocol suggested by Cola and Paris [30] to teleport a two-qubit system via a single quantum channel. This protocol based on using a single entangled two-qubit pair, additional qubit introduced by the receiver and the transmission of three classical bits. In our contribution, the users Alice and Bob share the generated partial entangled state Eq. (6). Alice is given unknown state defined by  $\rho_{in} = |\psi_{in}\rangle\langle\psi_{in}|$  where,

$$|\psi_{in}\rangle = \cos \theta |10\rangle + e^{i\varphi/2} \sin \theta |01\rangle, \tag{9}$$

with  $0 \leq \theta \leq \pi$  and  $0 \leq \varphi \leq 2\pi$ . The aim of Alice is to send this state to Bob using Eq. (6). To implement this process, the users follow Cola and Paris protocol [30]. At the end of this process, Bob will get the state [31]:

$$\rho_{Bob} = \sum_{\mu\nu} P_{\mu\nu} (\sigma_\mu \otimes \sigma_\nu) \rho_{in} (\sigma_\nu \otimes \sigma_\mu), \tag{10}$$

where  $P_{\mu\nu} = Tr[E^\mu \rho_{af}] Tr[E^\nu \rho_{af}]$ ,  $\sum_{\mu\nu} P_{\mu\nu} = 1$ , and  $\sigma_{\mu,\nu}$

$(\mu, \nu = 0, x, y, z)$  are the three components of the Pauli

operators and  $\sigma_0$  is the identity operator. The operators  $E^i$ ,  $i = 1, 2, 3, 4$  are defined as,

$$\begin{aligned} E^0 &= |\psi^-\rangle\langle\psi^-|, & E^1 &= |\phi^-\rangle\langle\phi^-|, \\ E^2 &= |\phi^+\rangle\langle\phi^+|, & E^3 &= |\psi^+\rangle\langle\psi^+|, \end{aligned}$$

where  $|\psi^\pm\rangle = \frac{1}{\sqrt{2}}(|01\rangle + |10\rangle)$  and  $|\phi^\pm\rangle = \frac{1}{\sqrt{2}}(|00\rangle + |11\rangle)$  are Bell states [12]. In the two dimensional basis set  $\{|n, g\rangle, |n, e\rangle, |n+1, g\rangle, |n+1, e\rangle\}$ , Bob's state may be written explicitly as,

$$\rho_{Bob} = \begin{pmatrix} \varrho_{11} & 0 & 0 & 0 \\ 0 & \varrho_{22} & \varrho_{23} & 0 \\ 0 & \varrho_{32} & \varrho_{33} & 0 \\ 0 & 0 & 0 & \varrho_{44} \end{pmatrix}, \tag{11}$$

where,

$$\begin{aligned} \varrho_{11} &= (\rho_{11} + \rho_{44})(\rho_{22} + \rho_{33}) \sin(2\theta) \cos(\varphi/2), \\ \varrho_{22} &= (\rho_{23} + \rho_{32})^2 \sin^2(\theta), \\ \varrho_{23} &= (\rho_{22} + \rho_{33})^2 \cos(\theta) \sin(\theta) e^{i\varphi/2} + (\rho_{11} + \rho_{44})^2 \cos(\theta) \sin(\theta) e^{-i\varphi/2}, \\ \varrho_{32} &= (\rho_{22} + \rho_{33})^2 \cos(\theta) \sin(\theta) e^{-i\varphi/2} + (\rho_{11} + \rho_{44})^2 \cos(\theta) \sin(\theta) e^{i\varphi/2}, \\ \varrho_{33} &= (\rho_{23} + \rho_{32})^2 \cos^2(\theta), \\ \varrho_{44} &= \rho_{11}. \end{aligned} \tag{12}$$

Now, if we consider the effect of a post partial measurement, Bob gets the teleported state  $\rho_{out}^A$  out whose three Bloch vector components are

$$\begin{aligned} s_x &= \sin(\theta) \cos(\varphi)[\rho_{22} + \rho_{33}]^2 + (\rho_{11} + \rho_{44})^2, \\ s_y &= 2 \sin(\varphi)[(\rho_{11} + \rho_{44})^2 - (\rho_{22} + \rho_{33})^2], \\ s_z &= -4 \cos(\theta)[\Re(\rho_{23})]^2, \end{aligned} \tag{13}$$

where  $\rho_{ij}$  given by Eq. (7)

### 3.2 Fisher information

In the estimation theory, the quantum Fisher information plays a central role. There are some parameters may cannot be quantified directly, so quantum Fisher information can be used to estimate these parameters. QFI is formally generalized from the classical one, and there are several variants of quantum versions of Fisher information, among which the one that based on the symmetric logarithmic derivative operator has been used most widely.

- *Fisher information of two-qubit system*

Assume that we have a two-qubits system which depends on a parameter,  $\kappa$ , then the amount of Fisher information that encoded in the parameter  $\kappa$  is defined as [8, 10]

$$\mathcal{F}_\kappa = Tr[\rho_\kappa \mathcal{L}_\kappa^2] = Tr[(\partial_\kappa \rho_\kappa) \mathcal{L}_\kappa], \tag{14}$$

where  $\mathcal{L}_\kappa$  is the so-called symmetric logarithmic derivative, which is determined by  $\partial_\kappa \rho_\kappa = (\mathcal{L}_\kappa \rho_\kappa + \rho_\kappa \mathcal{L}_\kappa)/2$  with  $\partial_\kappa = \partial/\partial\kappa$ . Making use of the spectrum decomposition, one can diagonalize the matrix as  $\rho_\kappa = \sum_n \lambda_n |\psi_n\rangle\langle\psi_n|$ . And then the QFI can be rewritten as [32]

$$\mathcal{F}_\kappa = \sum_n \frac{(\partial_\kappa \lambda_n)^2}{\lambda_n} + \sum_n \lambda_n \mathcal{F}_{\kappa,n} - \sum_{n \neq m} \frac{8 \lambda_n \lambda_m}{\lambda_m + \lambda_n} |\langle\psi_n|\partial_\kappa \psi_m\rangle|^2, \tag{15}$$

where  $\mathcal{F}_{\kappa,n}$  is the QFI for pure state  $|\psi_n\rangle$  with the form  $\mathcal{F}_{\kappa,n} = 4[|\langle\partial_\kappa \psi_n|\partial_\kappa \psi_n\rangle - |\langle\psi_n|\partial_\kappa \psi_n\rangle|^2]$ .

- *Fisher information of a single-qubit*

It is well known that a single qubit state  $\rho$ , may be defined by its Bloch vector as  $\rho = \frac{1}{2}(1 + \vec{s} \cdot \hat{\sigma})$  in the Bloch sphere representation, where  $\vec{s} = (s_x, s_y, s_z)$  is the real Bloch vector and  $\hat{\sigma} = (\hat{\sigma}_x, \hat{\sigma}_y, \hat{\sigma}_z)$  denotes the Pauli matrices. According to Ref. [33], a simple and explicit expression of QFI could be obtained in terms of the Bloch sphere representation  $\mathcal{F}_\kappa$

$$\mathcal{F}_\kappa = \begin{cases} |\partial_\kappa \vec{s}|^2 + \frac{(\vec{s} \cdot \partial_\kappa \vec{s})^2}{1 - |\vec{s}|^2}, & \text{if } |\vec{s}| < 1 \\ |\partial_\kappa \vec{s}|^2. & \text{if } |\vec{s}| = 1 \end{cases}$$

From the perspective of parameter estimation, the larger QFI represents the higher estimation precision in general. Hence, how to improve the QFI becomes a key problem to be solved. Making use of quantum resources such as coherence, entanglement and so on, one can find that QFI of quantum systems can provide much more sensitivity than the classical ones.

## 4 Estimation of the teleported parameters

It is clear that, the initial teleported information is encoded in the weight and phase parameters of the state (9). In the following we estimate these parameters by evaluating the corresponds quantum Fisher information of the initial teleported state.

### 4.1 Estimating the weight parameter $\theta$

We estimate the initial weight parameter using two different methods: the first, when we consider a single qubit is teleported by tracing out the first qubit from the final teleported state. The second by estimating it from the total teleported state. Moreover, we discuss the sensitivity of the estimation degree to the amplitude of the Bloch vector and the purity of the two qubit teleported state. In addition, we investigate the effect of the number of photons inside the cavity on the estimation degree of the weight parameter.

Figure 1a describes the behavior of the quantum Fisher information with respect to the weight parameter  $\mathcal{F}_\theta^q$ , using the first method, namely, using the quantum Fisher information that contained in the teleported single qubit. It is assumed that, the initial teleported state is prepared with a phase  $\varphi = \pi$ . This means that,  $|\psi_{in}\rangle = \cos \theta |10\rangle - \sin \theta |01\rangle$  and according to Eq. (13), the final state is polarized in y and z directions, namely  $\vec{s} = (0, s_y, s_z)$ . Moreover, the atomic-field system is initially prepared in a non-resonance case, where we set  $\delta = 0.5$ .

The general behavior shows that, the maximum values of Fisher information depend on the initial weight angle  $\theta$  and the dimensionless interaction time  $\tau = gt$ . As it is displayed in Fig. 1a, the Fisher information  $\mathcal{F}_\theta^q$  increases gradually to reach its maximum value for the first time at  $\tau = 4$ . For further values of the interaction time,  $\mathcal{F}_\theta^q$  decreases gradually. However, this behavior is repeated periodically. The effect of the initial weight parameter shows that, Fisher information decreases gradually to its minimum value at  $\theta = \pi/2$ . This behavior changes for  $\theta \in [3\pi/4, \pi]$ , where the Fisher information increases to reach its maximum bounds at  $\theta = \pi$ .

Figure 1b shows the behavior of the amplitude of the Bloch vector, where the non-resonance case is considered.

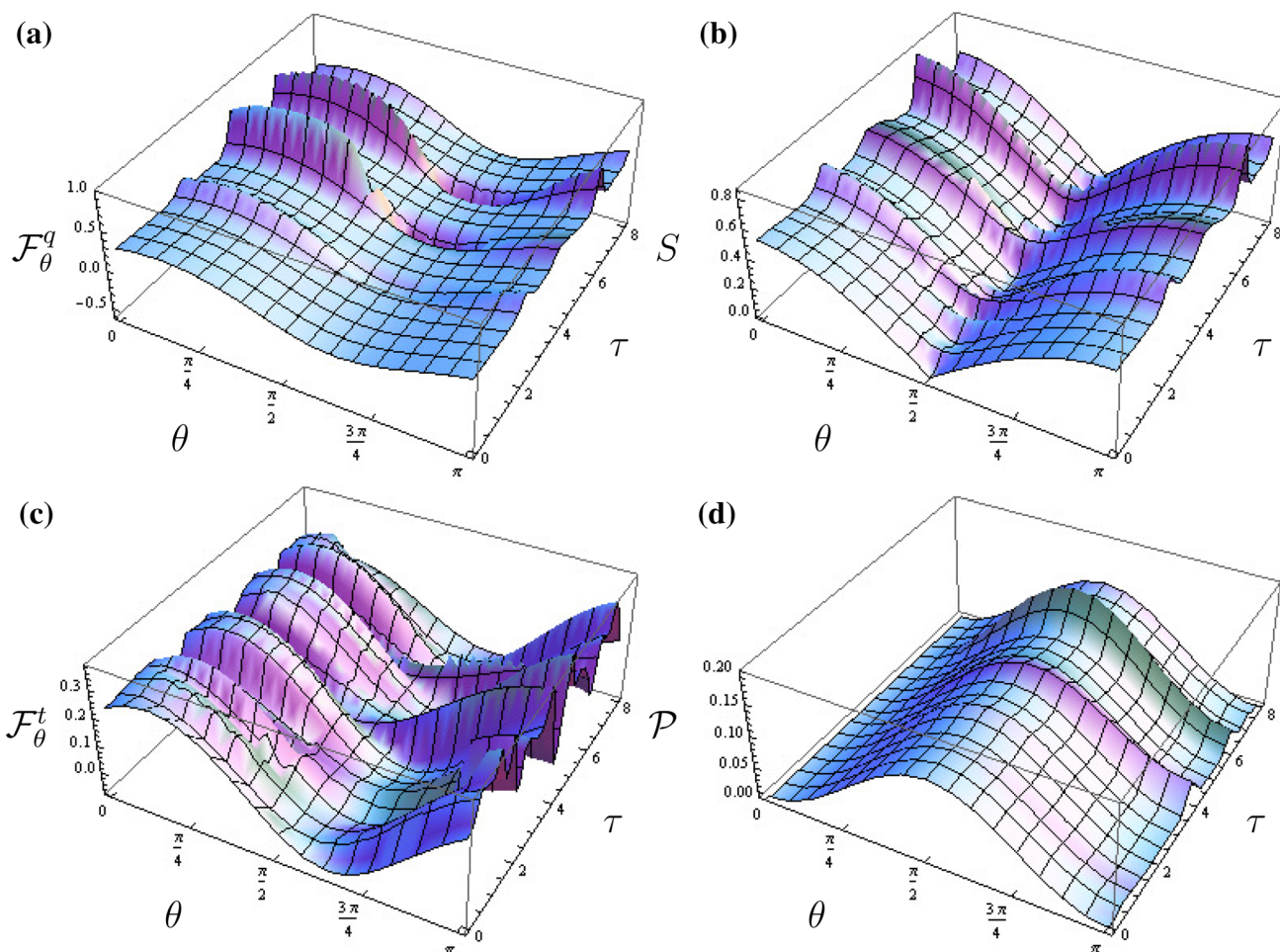


**Fig. 1** **a** The quantum Fisher information  $\mathcal{F}_\theta^q$ , of the single teleported qubit, **b** the Bloch vector  $S$  of the single qubit, **c**  $\mathcal{F}_\theta^t$  with respect to the total teleported state, **d** the purity of the teleported state,  $\mathcal{P}$  where, the non-resonance case is considered, with  $\delta = 0.5$ ,  $\varphi = \pi$  and  $n = \bar{n} = 2$

The behavior of the Bloch vector is similar to that predicated for the quantum Fisher information, namely  $S$  of the final state of the single qubit is periodically maximized. The lowest bounds of amplitude of the Bloch vector are displayed at  $\theta = \pi/2$ , namely the initial state is initially prepared in the state  $|\psi_{in}\rangle = e^{i\varphi}|01\rangle$ . For larger values of  $\theta$ , the amplitude of the Bloch vector increases suddenly to reach its maximum values at  $\theta = \pi$ .

In Fig. 1c, we display the behavior of the quantum Fisher information for the total teleported state, Eq. (12),  $\mathcal{F}_\theta^t$ . It is clear that, the behavior is similar to that predicated for the single qubit (Fig. 1a), but the maximum bounds are smaller. Moreover, the decay rate is larger than that displayed for the single qubit. In addition, the minimum bounds of  $\mathcal{F}_\theta^t$  are displayed around  $\theta = \pi/2$ . The periodical time is smaller than that displayed in Fig. 1a for the single qubit.

The purity of the final teleported state is displayed in Fig. 1d, where at  $\tau = 0$  and  $\theta = 0$ , the purity  $\mathcal{P}$  is zero. As  $\theta$  is increased in the interval  $[0, \pi/2]$ , the purity increases

gradually to reach its maximum values at  $\theta = \pi/2$ . For further values of  $\theta$ , the purity decreases gradually to completely vanish at  $\theta = \pi$ .

From Fig. 1, one may conclude that the possibility of estimating the weight parameter of the teleported state increases as the amplitude of the Bloch vector of the single qubit or the purity of the total teleported state increases. One can estimate the initial weight parameter with large degree by estimating it using the single teleported qubit.

In Fig. 2, we investigate the behavior of the quantum Fisher information, the amplitude of the Bloch vector and the purity of the total teleported state for different initial state settings, where we set that  $\varphi = \pi/2$ . This means that, the initial state is prepared in the state  $|\psi_{in}\rangle = \cos \theta|10\rangle + \frac{1+i}{\sqrt{2}} \sin \theta|10\rangle$  and the final state is polarized in  $y$  and  $z$  directions, namely  $\vec{s} = (0, s_y, s_z)$ . In Fig. 2a, the behavior of the quantum Fisher information  $\mathcal{F}_\theta^q$  is displayed, where it displays that the maximum bounds are

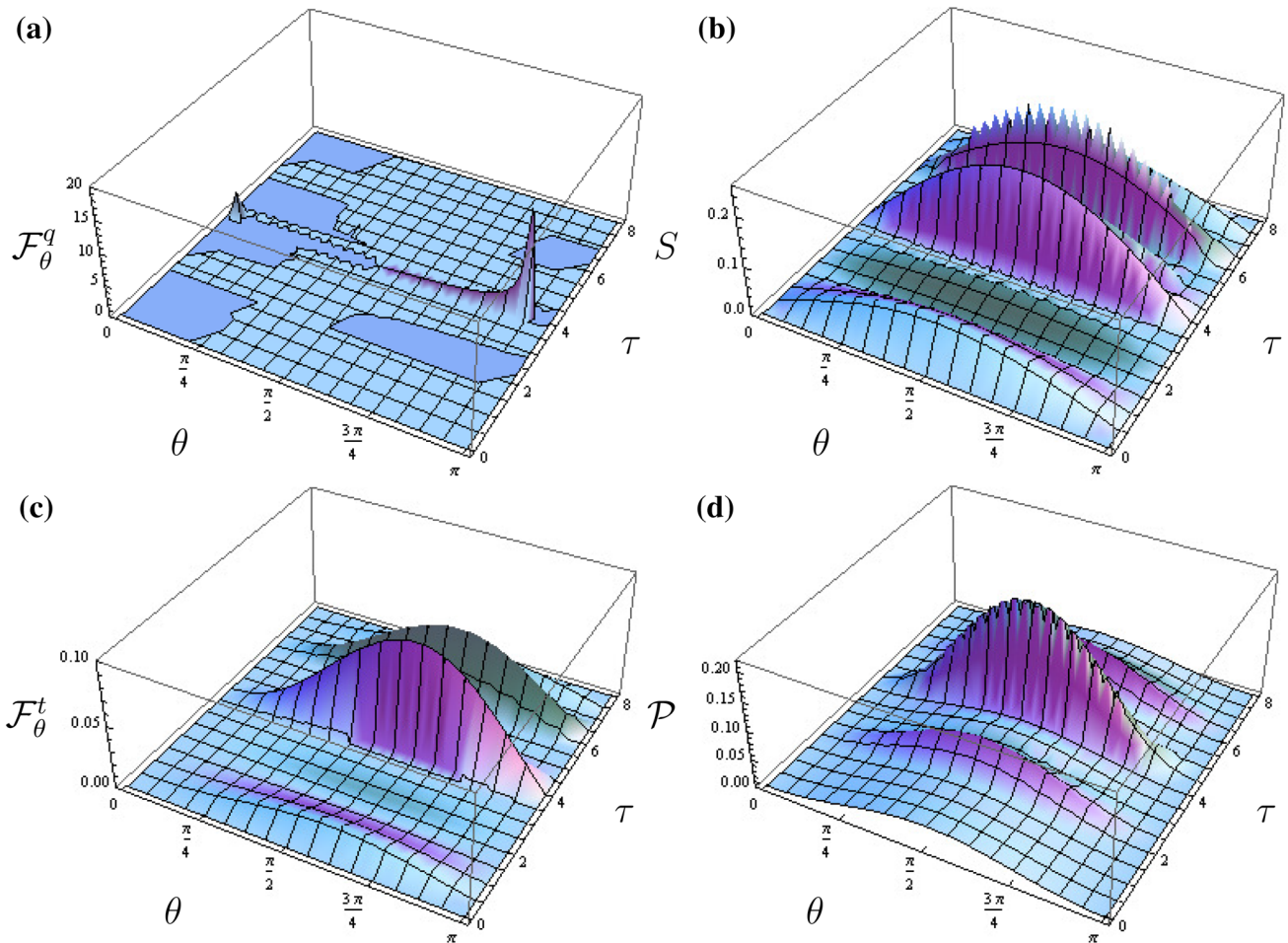


**Fig. 2** The same as Fig. 1, but  $\varphi = \pi/2$

very large compared with that displayed at  $\phi = \pi$ . Moreover, many frozen areas are displayed of the quantum Fisher information. Figure 2b, shows the behavior of the amplitude of the Bloch vector  $S$  for the single qubit. The general behavior, the upper bounds are smaller than that displayed in Fig. 1b. The maximum bounds are reached periodically. The estimation of the weight parameter by quantifying the Fisher information of the teleported two-qubit state is displayed in Fig. 2c. In general, the possibility of estimating the weight parameter  $\theta$  is smaller than that displayed in Fig. 1c. This indicates that, the initial phase has a clear effect on the estimation degree of the weight parameter. The possibility of freezing the Fisher information increases for this initial state settings. Similar behavior is displayed for the purity, where as it displayed in Fig. 2d, the maximum bounds are smaller than those displayed in Fig. 1d.

Again as the purity of the teleported state increases, the possibility of estimating the weight parameter increases.

Moreover, one can freeze the quantum Fisher information by controlling the phase of the initial teleported state.

Figure 3 describes the behavior of the four physical quantities,  $F_\theta^q$ ,  $S$ ,  $F_\theta^t$  and the purity  $\mathcal{P}$ , in the resonance case between the atom and the field, namely we set the dimensionless parameter  $\delta = 0$ . It is clear that, as it depicted in Fig. 3a, the maximum bounds of  $F_\theta^q$  are larger than those displayed in Fig. 1a (non-resonance case). In addition, as the initial weight parameter,  $\theta$  increases, the quantum Fisher information  $F_\theta^q$  decreases gradually, where the minimum bounds are displayed at  $\theta \in [\pi/2, 3\pi/4]$ , while the maximum peaks appear periodically as the  $\tau$  increases. However, the decay rate is smaller than that shown for the non-resonance case. The behavior of the Bloch vector of the teleported state is displayed in Fig. 3b. The behavior is completely different from that displayed in Fig. 1b, where the maximum bounds are displayed at  $\theta = \pi$ , while the minimum values are depicted at  $\theta = 0, \pi$ . In addition, similarly to Fig. 1b, the maximum bounds are displayed periodically at larger values of the dimensionless time  $\tau$ . The quantum

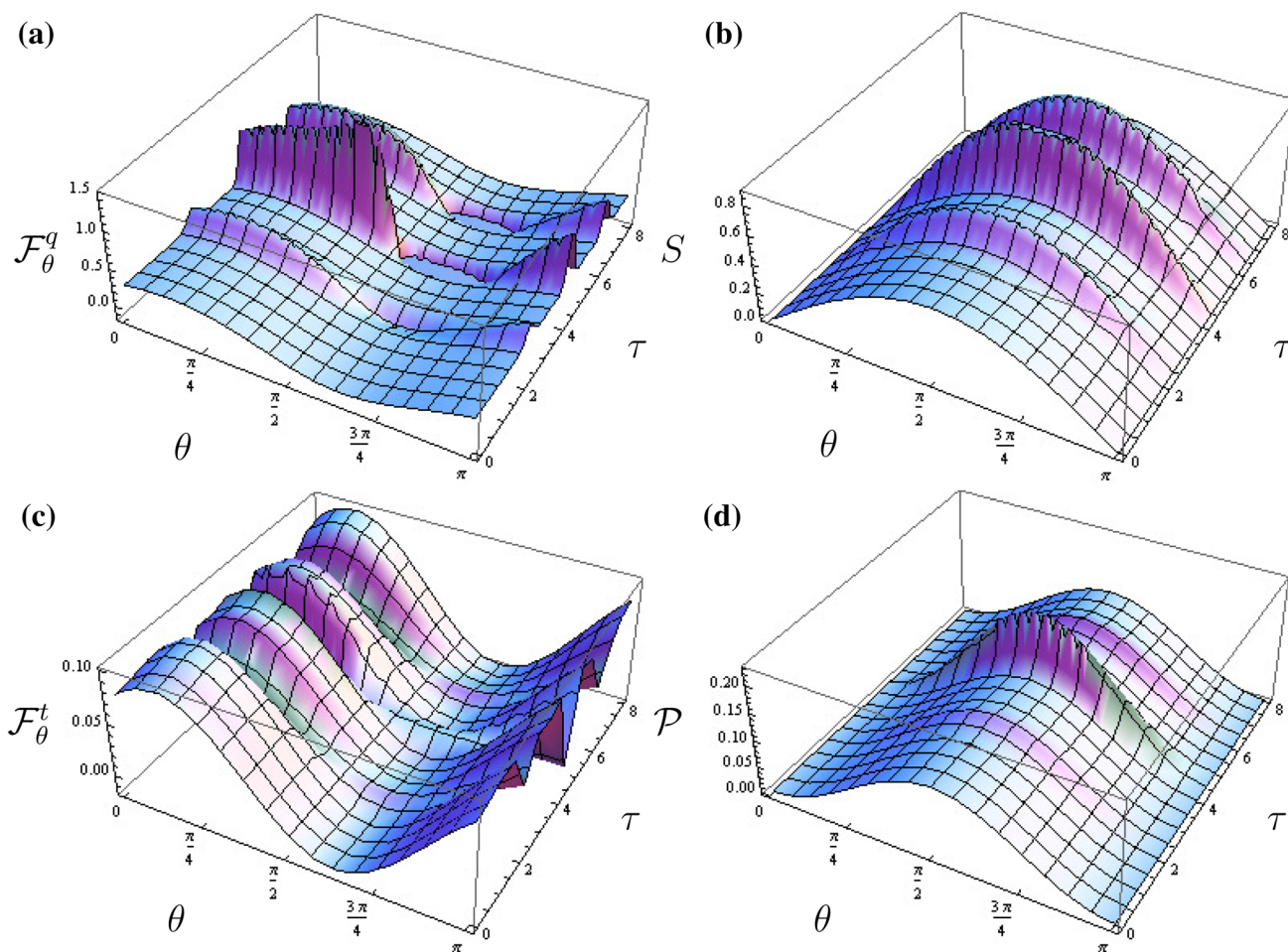


**Fig. 3** The quantum Fisher information  $\mathcal{F}_\theta^q$ , of the single teleported qubit, **b** the Bloch vector  $S$  of the single qubit, **c**  $\mathcal{F}_\theta^t$  with respect to the total teleported state **d** the purity of the teleported state,  $\mathcal{P}$  where, the resonance case  $\delta = 0$  with  $\varphi = \pi$  and  $n = \bar{n} = 2$

Fisher information  $\mathcal{F}_\theta^q$  is displayed in Fig. 3c. In general, it behaves similarly to the non-resonance case, but the upper bounds are smaller compared with those displayed in Fig. 1c. In addition, as it is displayed in Fig. 3d, the purity increases as the initial phase  $\varphi$  increases to reach its maximum values at  $\varphi = \pi/2$ . However, at further values of  $\varphi \in [\pi/2, \pi]$ , the purity decreases. It is clear that, it shows the same behavior that depicted for the non-resonance case.

In Fig. 4, we display the effect of a different initial phase settings ( $\varphi = \pi/2$ ) on the behavior of the quantum Fisher information  $\mathcal{F}_\theta^q$  and  $\mathcal{F}_\theta^t$ . It is clear that, one can not estimate the weight parameter or the estimation degree is almost zero. This means that, the quantum Fisher information is completely frozen. On the other hand, as it is displayed in Fig. 4b, the amplitude of the Bloch vector increases periodically as the dimensionless time increases and at some intervals of time, the teleported single state turns into a maximum pure state. However, although it is impossible to estimate the

teleported weight parameter with larger estimation degree, the teleported state keeps with its local information. In addition, from Fig. 4d, the purity in some interval of time is non-zero and increases as  $\tau$  increases. Again, this indicates that, the teleported two-qubit state has some local information.

From Figs. 1 and 3, one may conclude that, the possibility of estimating the weight parameter  $\theta$  depends on the detuning parameter. In the non-resonance case, the estimation degree of the weight parameter is larger than that displayed for the resonance case. The initial weight settings  $\theta$  has the same effect on resonance and non-resonance case, where the minimum bounds are displayed at  $\theta = \pi/2$ . The initial phase may be considered as a decoherence parameter as it displayed from Figs. 2 and 4, where the Fisher information is frozen at different interval time for the non-resonance case. However, the quantum Fisher information is completely frozen for the resonance case.

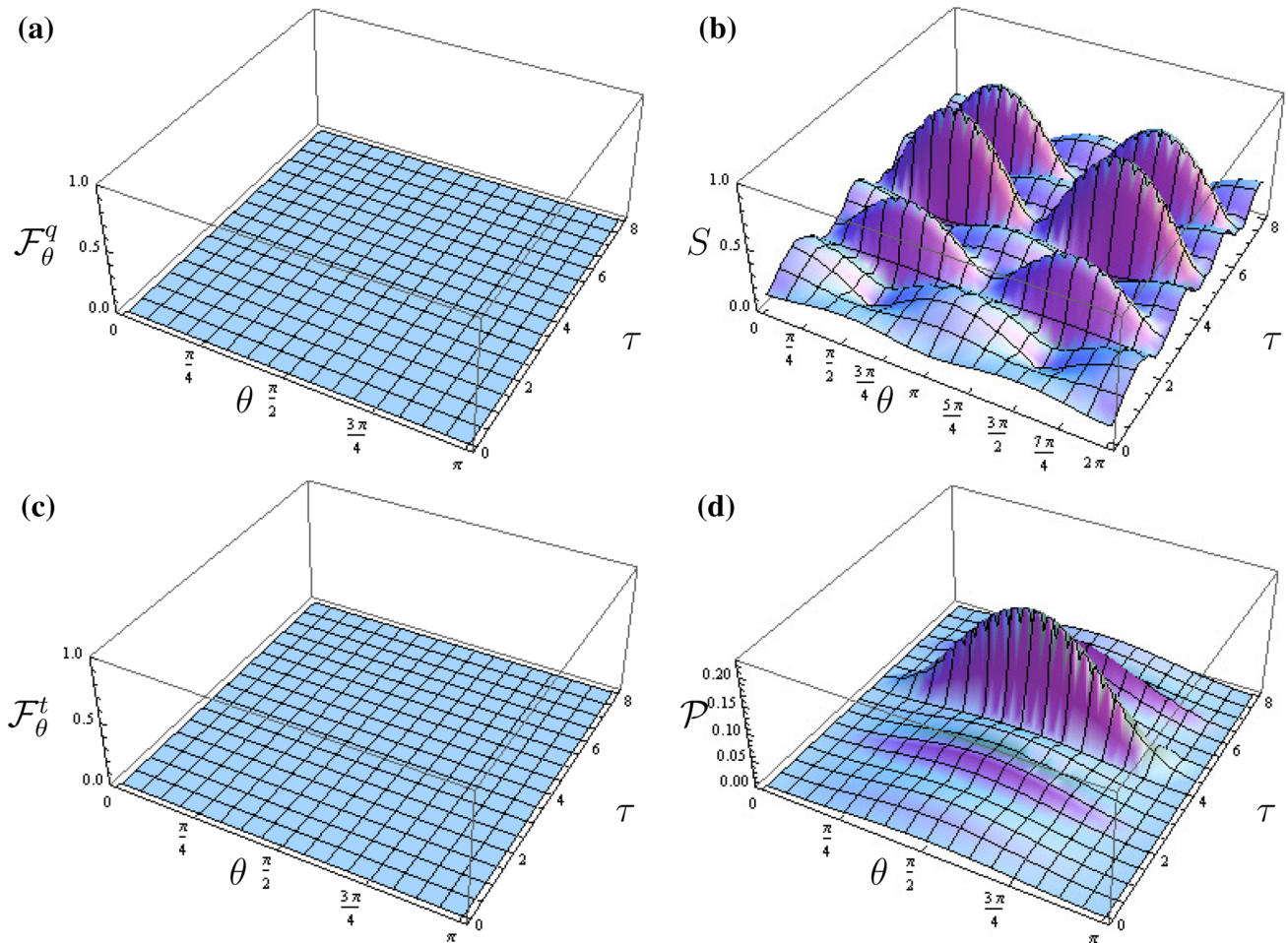


Fig. 4 The same as Fig. 3 but the initial phase  $\varphi = \pi/2$

To investigate the effect of the number of photons on the four physical quantities, we plot Fig. 5, where we set the initial phase  $\varphi = \pi/2$  and the number of photon  $n = 4$ . It is clear that, the number of photons has no effect on the estimation degree of the weight parameter, where the quantum Fisher information is almost frozen as it is depicted from Fig. 5a, c. On the other hand, the amplitude of the Bloch vector of the single teleported state increases as  $\tau$  increases. Moreover, the initial weight has no effect where, the periodic behavior is displayed between a minimum and maximum bounds. Fig. 5d shows that the purity of the teleported two-qubit state increases periodically as  $\tau$  increases. Comparing Figs. 4b and 5b, one can see that the larger numbers of photon inside the cavity increase the oscillations number between the maximum and minimum bounds,

From Figs. 4a, c and 5a, c, we can see that, the Fisher information is completely frozen and the estimation degree is almost zero, but the amplitude of the Bloch vector as well as the purity of the teleported two-qubit state are not vanish. This means that, the teleported state has its own local

information. Namely, one can not estimate the parameters which contain all the teleported information.

We have shown that, one can freeze the quantum Fisher information by choosing a particular values of the initial phase. However, at some values of the phase, the quantum Fisher information does not completely frozen as it shown at  $\varphi = \pi$ . In Fig. 6a, b, we display the frozen region of the quantum Fisher information,  $\mathcal{F}_\theta^q$  and  $\mathcal{F}_\theta^t$  respectively, where we set the detuning parameter  $\delta = 0.5$ . The degree of brightness indicates the estimation degree of the weight parameter. It is clear, that the frozen areas of the quantum Fisher information of the teleported two qubit state are larger than those displayed for the single teleported state. The degree of frozen decreases as the initial weight increases. Figure 6c, d show the effect of the larger detuning parameter ( $\delta = 1$ ), on the frozen areas. It is clear that, the behavior is similar to that displayed at  $\delta = 0.5$ . However, the upper bounds are smaller than those displayed in Fig. 6a, b. The frozen areas missed their symmetric and the deformation of these areas depicted clearly for  $\mathcal{F}_\theta^t$ .



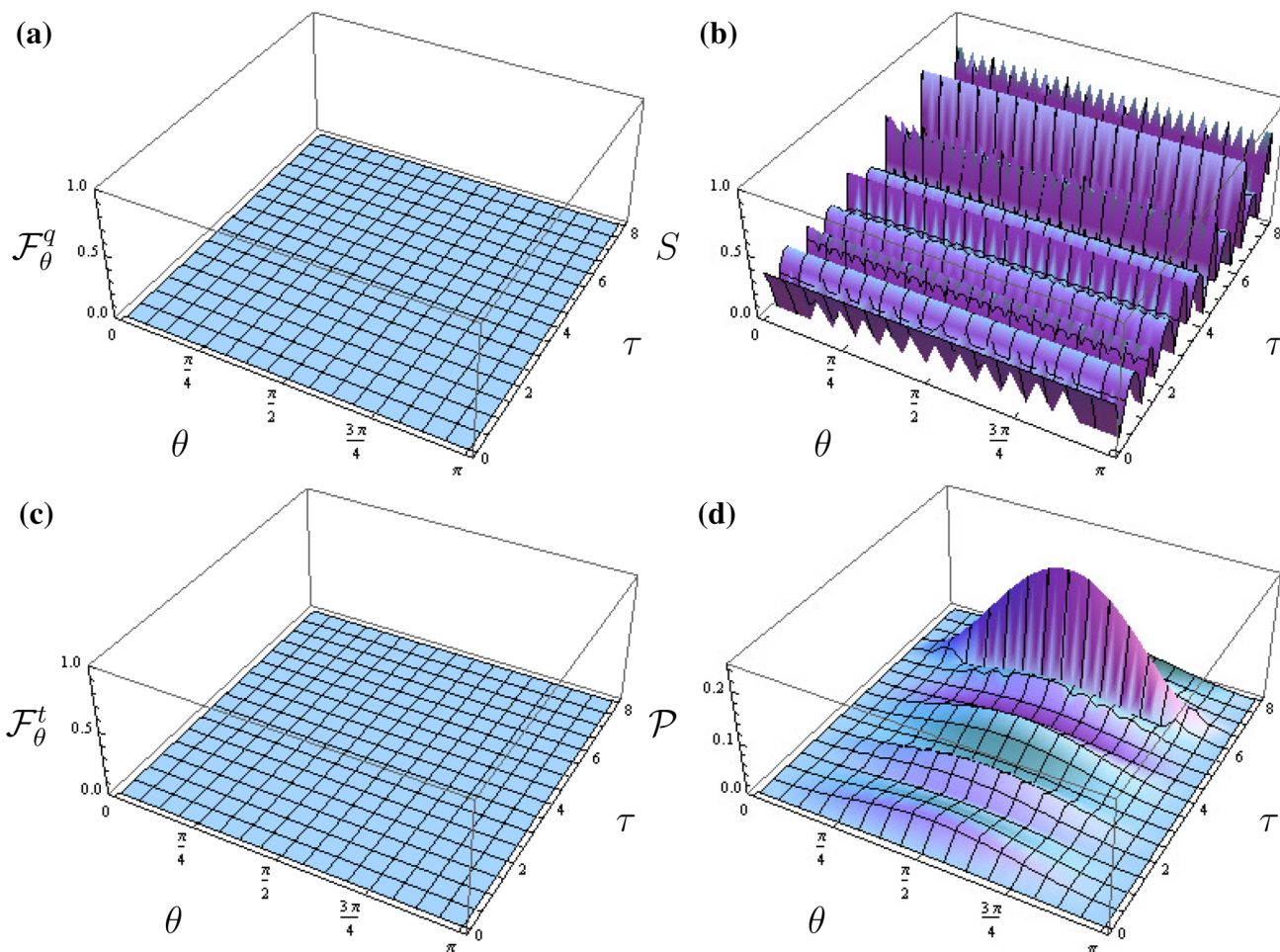


Fig. 5 The same as Fig. 4 but we set  $n = 4$  and  $\bar{n} = 2$

From Fig. 6, one may conclude that, the possibility of estimating the weight parameter decreases as the initial detuning between the atom and the cavity increases. Moreover, the sizes and the deformation of the frozen areas decrease at larger values of the detuning.

### 4.2 Estimating the phase parameter $\varphi$ .

In this section, we estimate the initial phase for the teleported single state and the teleported two-qubit state at different initial settings.

In Fig. 7, we consider the non-resonance case, where we set  $\delta = 0.5$ . Similarly to the Fisher information with respect to the weight parameter, the upper bounds are displayed periodically and the maximum values are depicted at larger values of the Bloch vector as it is shown from Fig. 7a, b. The phenomenon of the freezing, the sudden changes of the quantum Fisher information  $\mathcal{F}_\varphi^q$  are depicted periodically. The quantum Fisher information as well as the amplitude of the Bloch vector are independent from the initial phase.

The estimation degree of the phase parameter using the teleported two-qubit state is smaller than that obtained if one use the teleported single state. Similarly to that displayed of  $\mathcal{F}_\varphi^q$ , the  $\mathcal{F}_\varphi^t$  is independent of the initial phase as it is displayed from Fig. 7c. The phenomena of the sudden decreasing/increasing are depicted periodically.

Figure 8a, b describes the behavior of the quantum Fisher information of the single teleported qubit and the teleported two-qubit system. The general behavior displays that, the Fisher information reaches its maximum values periodically. As it is shown in Fig. 8a, b, the upper bounds of the quantum Fisher information  $\mathcal{F}_\varphi^q$  and  $\mathcal{F}_\varphi^t$  are displayed periodically. Moreover, the sudden changes of the quantum Fisher information is displayed. The maximum bounds are depicted at  $\varphi = \pi/2, 3\pi/2$ , where the estimation degree of  $\mathcal{F}_\varphi^q$  is larger than that depicted for  $\mathcal{F}_\varphi^t$ . From these results, one can show that, the possibility of estimating the phase parameter from the single teleported state is larger than that estimated using the teleported two-qubit state. In Fig. 8c, d, we investigate the effect of larger number of photons on the estimation

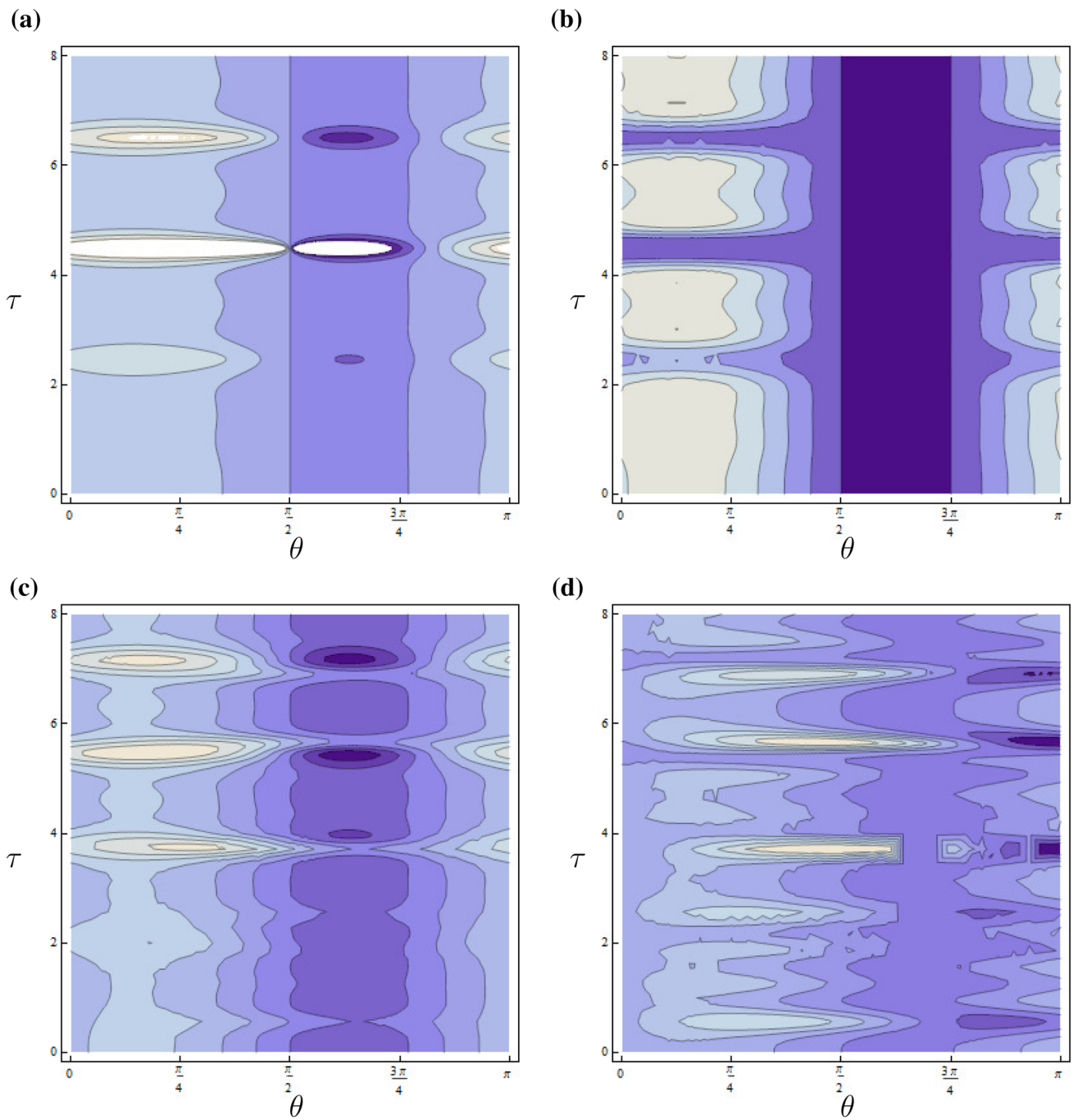


**Fig. 6** **a, c** The quantum Fisher information  $\mathcal{F}_\theta^q$  and **b, d**  $\mathcal{F}_\theta^l$  where  $\varphi = \pi$ ,  $n = \bar{n} = 2$  and  $\delta = 0.5, 1$  for **a, b** and **c, d**, respectively

degree, where we set  $n = 4$ . The behavior is similar to that displayed in Fig. 8a, b. But the number of peaks is larger than that displaced at smaller values of  $n$ . The minimum values are displayed around  $\pi/2$  and  $3\pi/2$  for  $\mathcal{F}_\theta^q$ , while the maximum bounds are shown around  $\pi/2$  and  $3\pi/2$  for  $\mathcal{F}_\theta^l$ .

From Figs. 7 and 8, one can conclude that, the maximum estimation degree of the phase parameter is displayed in the non-resonance case. The possibility of freezing the quantum

Fisher information in the resonance case is larger than that shown for the non-resonance case.

In Fig. 9, we investigate the effect of the detuning parameter on the quantum Fisher information. Figure 9 represents a contour graph in the space of  $(\tau, \varphi)$  of  $\mathcal{F}_\theta^q$  and  $\mathcal{F}_\theta^l$ , where we set the initial detuning parameter  $\delta = 0.5$ . This graph displays the frozen areas of the quantum Fisher information. The dark regions indicate that the estimation

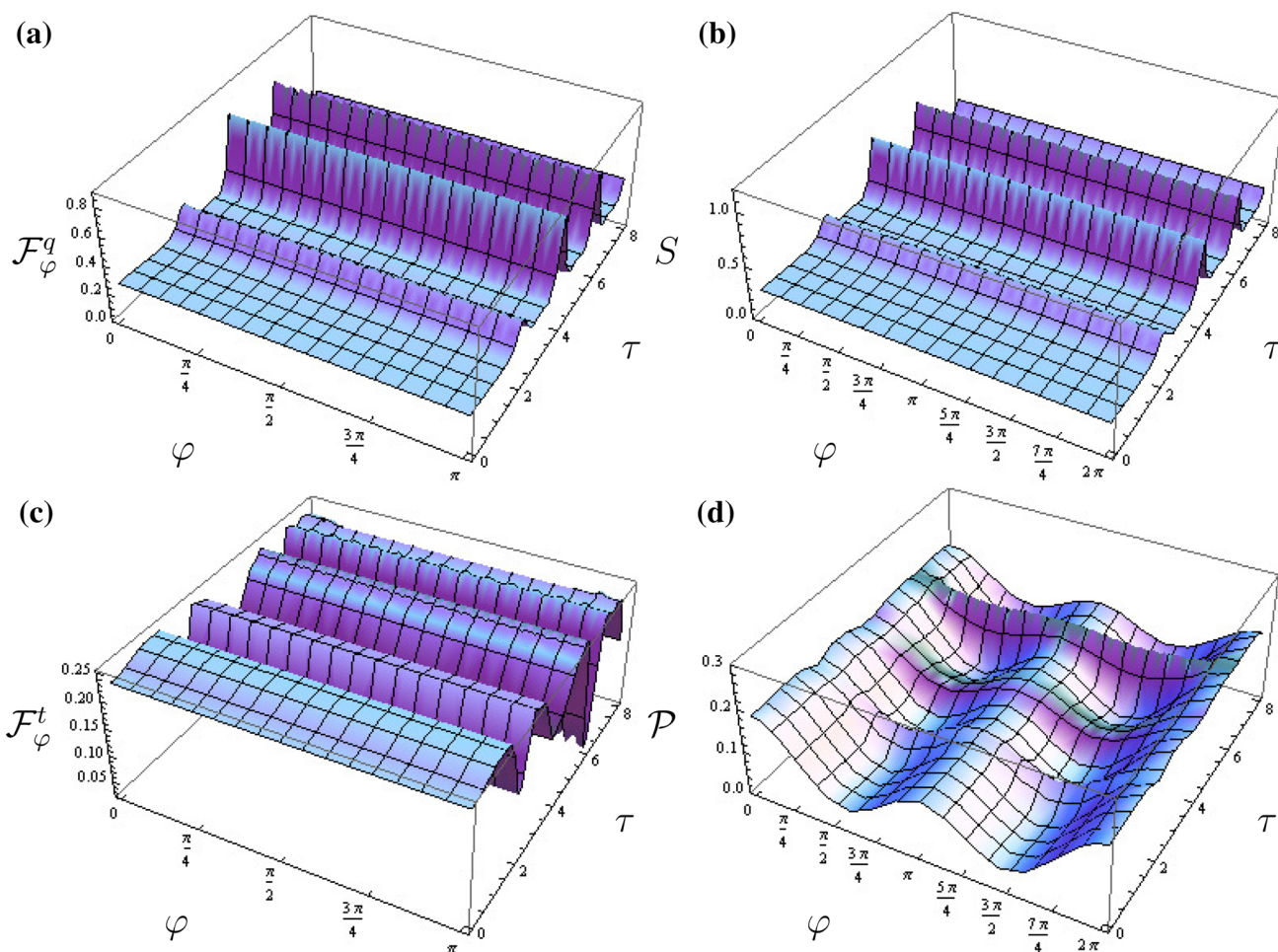


**Fig. 7** **a** The quantum Fisher information  $\mathcal{F}_\varphi^q$ , of the single teleported qubit, **b** the Bloch vector  $S$  of the single qubit, **c**  $\mathcal{F}_\varphi^t$  with respect to the total teleported state **d** the purity of the teleported state,  $\mathcal{P}$  where, the non resonance case, when  $\delta = 0.5, \theta = \pi/2, n = 2$  and  $\tilde{n} = 2$

degree of the Fisher information is minimum. However, it is clear that, as the interaction time increases, some bright regions are appear, namely, one may estimate the quantum Fisher information with a large degree. From Fig. 9a, b, it is clear that, when  $\mathcal{F}_\varphi^q$  is estimated with a small degree, the estimation degree of  $\mathcal{F}_\varphi^t$  is large. Moreover, as the brightness areas appear for  $\mathcal{F}_\varphi^q$ , the darkness regions of  $\mathcal{F}_\varphi^t$  are predicated. The frozen dark/bright regions appear periodically and independent of the initial phase.

The effect of the larger values of the detuning parameter is displayed in Fig. 9c for  $\mathcal{F}_\varphi^q$  and Fig. 9d for  $\mathcal{F}_\varphi^t$ , where we set  $\delta = 1$ . It is clear that, the dark/bright regions appear periodically as  $\tau$  increases. As it displayed from Fig. 9c, the brightness degree of the frozen areas that represents  $\mathcal{F}_\varphi^q$  increases as  $\tau$  increases, while for  $\mathcal{F}_\varphi^t$  depends on the initial phase.

Figure 10, describes the frozen regions of the quantum Fisher information in the resonance case. The darkness/brightness degree of the frozen areas, indicates

the estimation degree of the quantum Fisher information. These regions appear periodically and the size of these regions decreases as the scaled time increases. The darkness regions, namely, the minimum estimation degree are depicted almost if the initial phase  $\varphi \in [0, \pi/4] \cup [\pi, 5\pi/4]$ , while the most brightness are predicated at  $\varphi \in [\pi/2, 3\pi/4] \cup [3\pi/2, 7\pi/4]$ .

However, these results are displayed at smaller values of the photons number inside the cavity, where we set  $n = 2$ . The effect of a large number of photons on the size of the frozen areas is displayed in Fig. 10c, d, where we set  $n = 4$ . From Fig. 10c, we can see that the number of the frozen areas increases as the photon number increases. The estimation degree of  $\mathcal{F}_\varphi^q$  increases and  $\mathcal{F}_\varphi^t$  decreases as the scaled interaction time  $\tau$  increases. The frozen bright/dark areas that are depicted for  $\mathcal{F}_\varphi^{q,t}$  are periodically depicted as  $\tau$  increases. However, the brightness degree of the frozen areas for  $\mathcal{F}_\varphi^q$  does not depend on the initial phase  $\varphi$ , while for that displayed for  $\mathcal{F}_\varphi^t$  increases as the initial phase  $\varphi$  increases

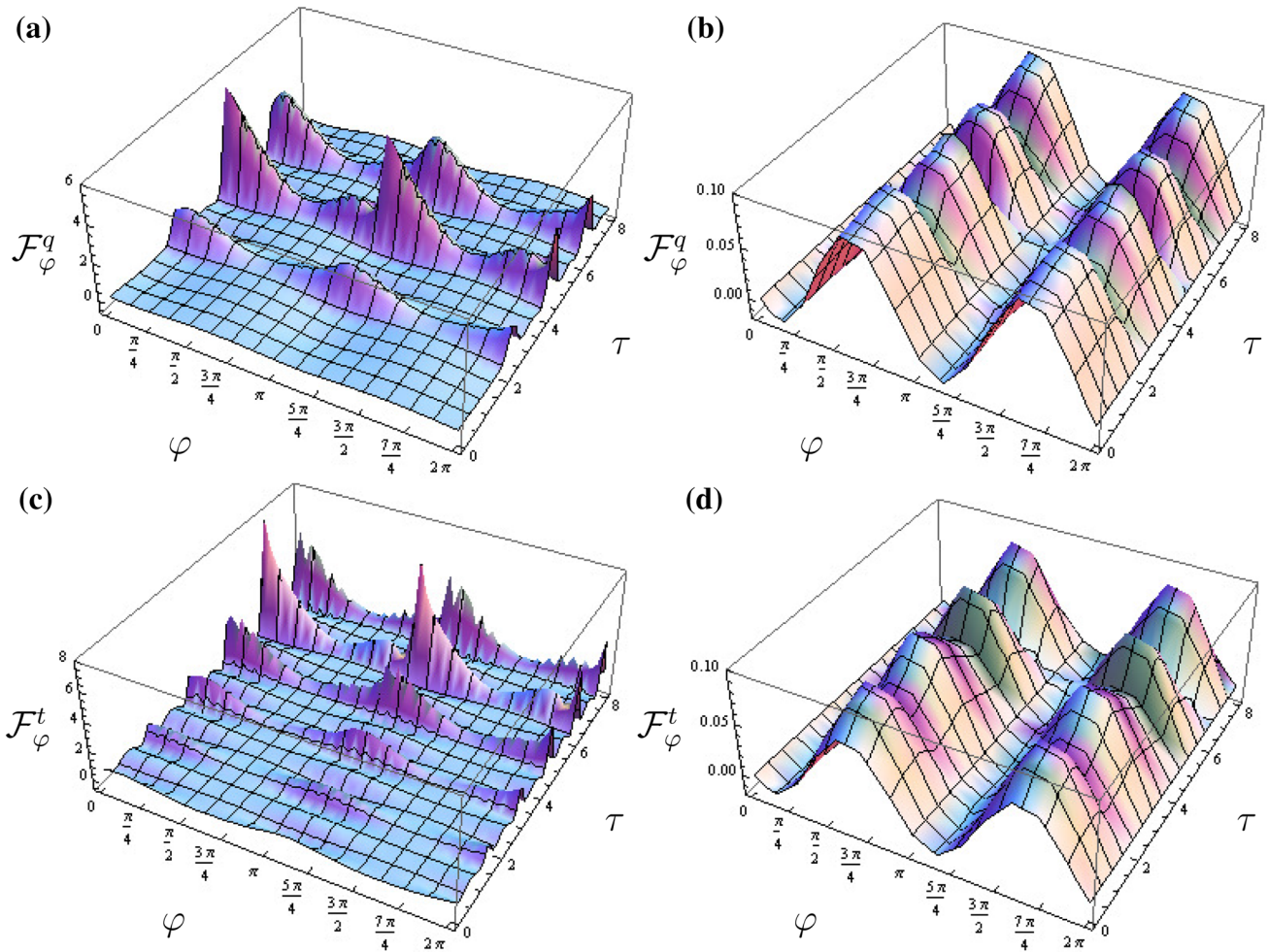


**Fig. 8** **a, b** The quantum Fisher information  $F_\varphi^q$ , of the single teleported qubit and **c, d** represents  $F_\varphi^t$  with respect to the total teleported state where,  $\delta = 0, \theta = \pi/2, \bar{n} = 2$  and **a, b**  $n = 2$ , **c, d**  $n = 4$

and the most brightness areas are centered around  $5\pi/4$  and  $7\pi/4$ . However, the most dark areas are displayed around  $\varphi \in [0, \pi/4] \cup [\pi, 5\pi/4]$  for  $F_\varphi^t$ , while for  $F_\varphi^q$  similarly but periodically with the bright regions.

### 5 Conclusion

In this contribution, we use a partial entangled state which is generated between a single atom and a single cavity mode, to teleport a two-qubit system between two users; Alice and Bob. The initial parameters of the teleported state; the weight and the phase parameters are estimated, by means of the teleported quantum Fisher information. These parameters are estimated from the teleported two-qubit state and the single qubit state. The relation between the purity of the teleported state and the quantum Fisher information is discussed. The effect of the initial detuning parameter and the

number of photons inside the cavity on the estimation degree of the initial teleported parameters is discussed.

Our results show that, the estimation degree of the parameters of the initial teleported state settings, increases as the amplitude of the Bloch vector of the single qubit and the purity of the total teleported state increases. The possibility of estimating the initial weight and the phase parameters by using a single qubit is larger than that displayed for the teleported two-qubit system. It is shown that, by controlling the initial state settings, the quantum Fisher information may be frozen, meanwhile, the teleported state keeps its local information. The frozen degree, dark/bright indicates the estimation degree of the teleported parameters.

The estimation degree depends on the initial parameters of the atomic-field system, where the possibility of estimating the teleported parameter in the resonance case is larger than that depicted for the non-resonance case. The upper and lower bounds of the quantum Fisher information are displayed periodically. The size of the frozen areas decreases

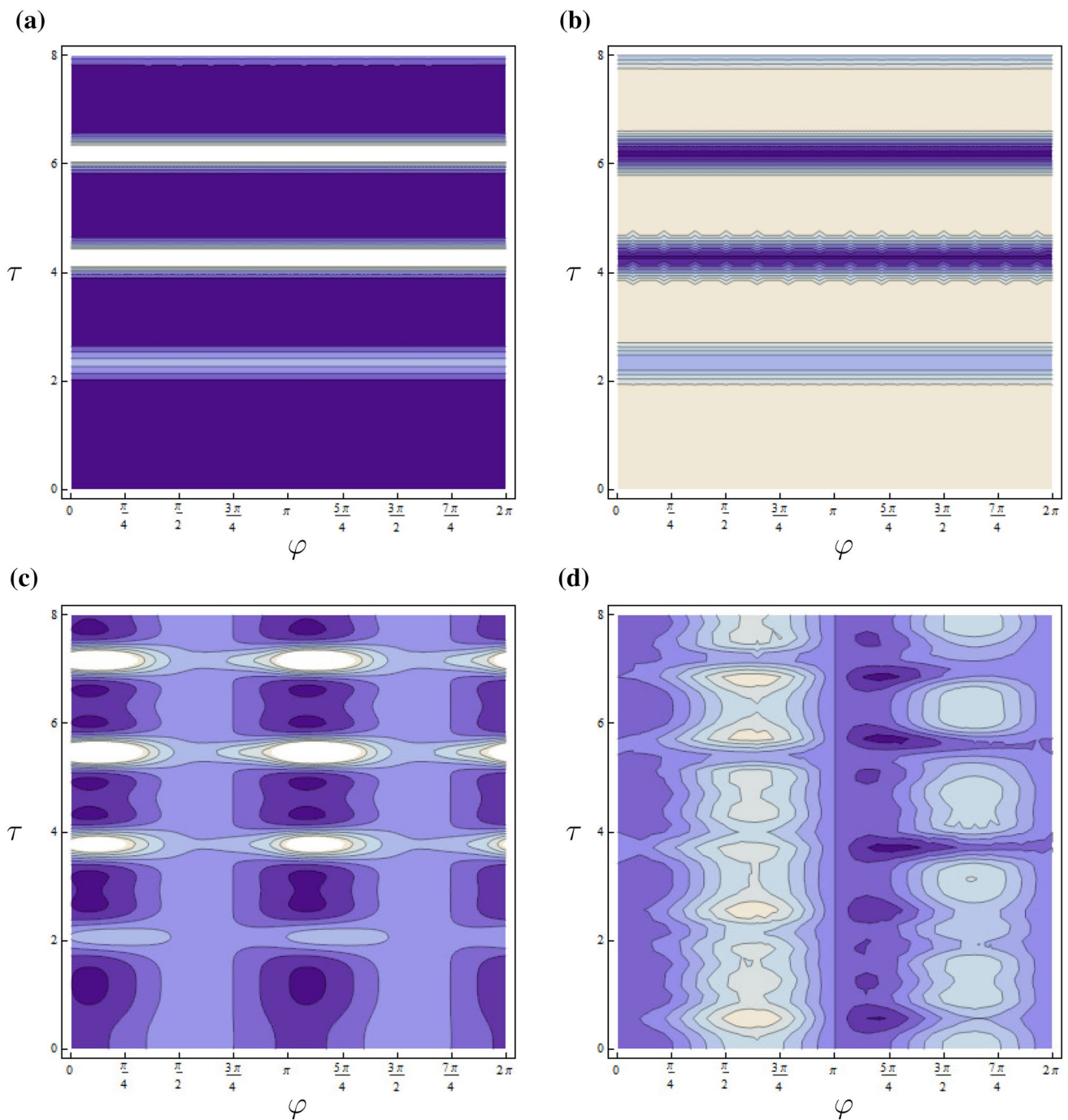


**Fig. 9** Contour graph for the Fisher information for the single qubit **(a, c)** and for the two qubit **(b, d)** with respect to the phase parameter with  $\theta = \pi/2, n = 2, \bar{n} = 2$  and **a, b**  $\delta = 0.5$ , **c, d**  $\delta = 1$

as the detuning parameter increases. The frozen areas of quantum Fisher information that are displayed at smaller values of the detuning parameter are regular and symmetric. However, as the detuning parameter increases, the frozen areas are deformed

The effect of the photons number inside the cavity is investigated, where the larger number of photons increases

the speed of oscillating the quantum Fisher information between their maximum and minimum bounds. It is shown, as one increases the number of photon inside the cavity, the upper bounds of the quantum Fisher information are larger than that displayed at smaller number of photons. The number of the frozen areas increases at the expense of their sizes.

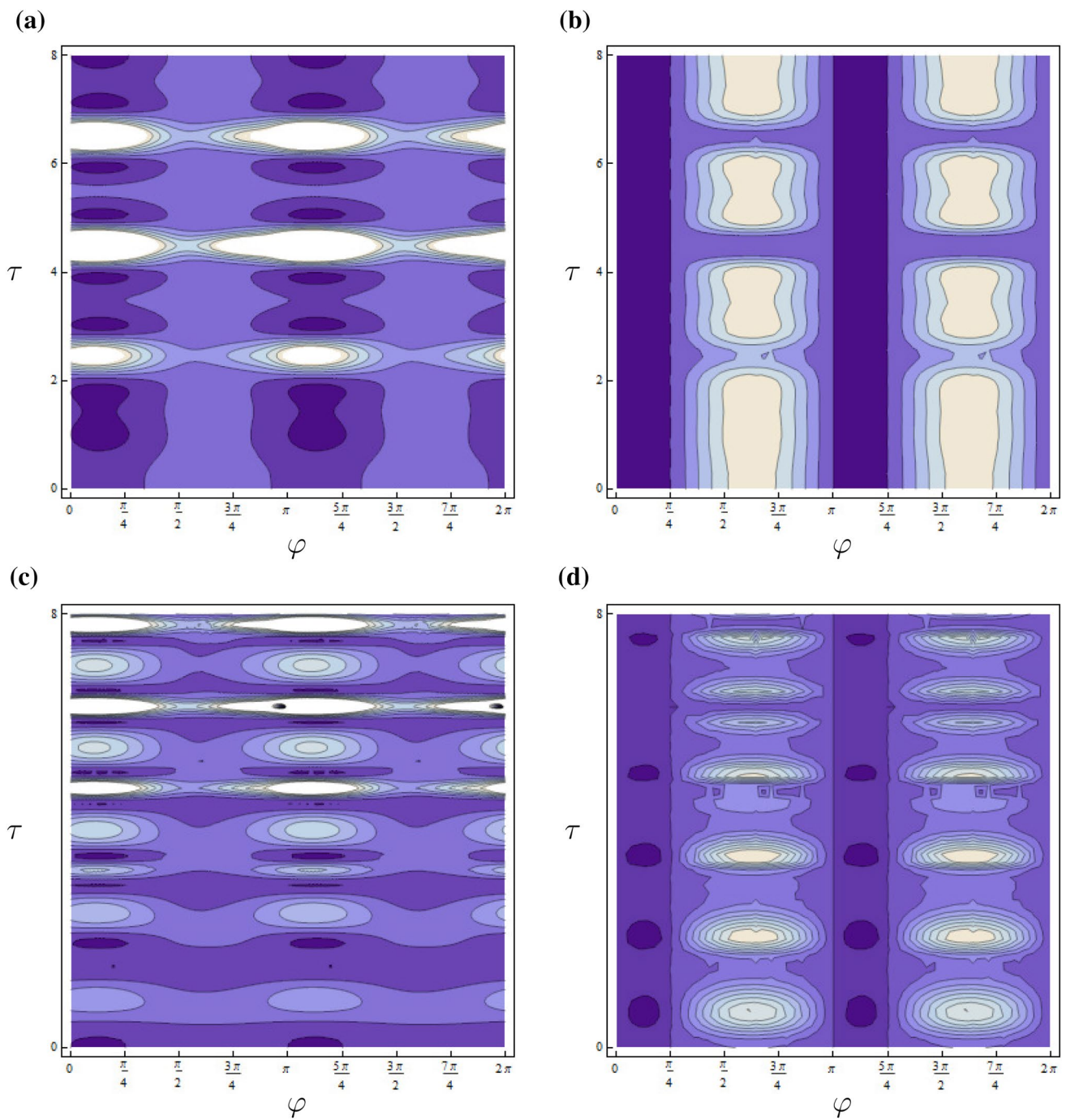


**Fig. 10** The figures **a**, **c** represent the Contour behavior of  $F_\varphi^q$  and **b**, **d** represent  $F_\varphi^l$  in resonance case, where  $\theta = \pi/2, \bar{n} = 2$  and  $n = 2$  for **a**, **b** and  $n = 4$  for **c**, **d**

In conclusion: it is possible to freeze the teleported parameters by controlling the initial atomic-field parameters and meanwhile the teleported state keeps its local information. These results may be useful in the context of secure quantum communication.

**Acknowledgements** A.E.A. acknowledges the hospitality of the Abdus Salam International Center for Theoretical Physics (Trieste, Italy).

## References

1. C.H. Bennett, G. Brassard, C. Crepeau, R. Jozsa, A. Peres, W.K. Wootters, Teleporting an unknown quantum state via dual classical and Einstein–Podolsky–Rosen channels. *Phys. Rev. Lett.* **70**, 1895 (1993)
2. D. Gottesman, I. Chuang, Quantum teleportation is a universal computational primitive. *Nature (London)* **402**, 390 (1999)
3. R. Ursin, Communications: quantum teleportation across the Danube. *Nature (London)* **430**, 849 (2004)
4. A. El Allati, Y. Hassouni, N. Metwally, Communication via an entangled coherent quantum network. *Phys. Scr.* **83**, 065002 (2011)
5. S.L. Braunstein, H.J. Kimble, Teleportation of continuous quantum variables. *Phys. Rev. Lett.* **80**, 869 (1998)
6. H. Takesue et al., Quantum teleportation over 100 km of fiber using highly efficient superconducting nanowire single-photon detectors. *Optica* **2**, 832 (2015)
7. A. El Allati, N. Metwally, Y. Hassouni, Transfer information remotely via noise entangled coherent channels. *Opt. Commun.* **284**, 519 (2011)
8. C.W. Helstrom, *Quantum Detection and Estimation Theory* (Academic, New York, 1976)
9. X.M. Lu, Z. Sun, X. Wang, S. Luo, C.H. Oh, Broadcasting quantum Fisher information. *Phys. Rev. A* **87**, 050302(R) (2013)
10. A.S. Holevo, *Probabilistic and Statistical Aspects of Quantum Theory* (North-Holland, Amsterdam, 1982)
11. W.K. Wootters, Statistical distance and Hilbert space. *Phys. Rev. D* **23**, 357 (1981)
12. M. Nielsen, I. Chuang, *Quantum Computation and Quantum Information* (Cambridge University Press, Cambridge, 2000)
13. V. Giovannetti, S. Lloyd, L. Maccone, Quantum metrology. *Phys. Rev. Lett.* **96**, 010401 (2006)
14. V. Giovannetti, S. Lloyd, L. Maccone, Advances in quantum metrology. *Nat. Photon.* **5**, 222 (2011)
15. S.L. Braunstein, C.M. Caves, Statistical distance and the geometry of quantum states. *Phys. Rev. Lett.* **72**, 3439 (1994)
16. J. Ma, Y.-X. Huang, X. Wang, C.P. Sun, Quantum Fisher information of the Greenberger–Horne–Zeilinger state in decoherence channels. *Phys. Rev. A* **84**, 022302 (2011)
17. Q. Zheng, Y. Uao, Y. Li, Optimal quantum channel estimation of two interacting qubit subject to decoherence. *Eur. Phys. J. D* **68**, 170 (2014)
18. F. Ozaydin, Quantum Fisher information of W States in Decoherence channels. *Phys. Lett. A* **378**, 3161 (2014)
19. W.G. You, G.Y. Neng, Z. Ke, Dynamics of quantum Fisher information in a two-level system coupled to multiple Bosonic reservoirs. *Chin. Phys. B.* **24**, 114201 (2015)
20. A.A. Altinats, *Ann. Phys.* **376**, 192 (2016)
21. N. Metwally, Estimation of teleported and gained parameters in a non-inertial frame. *Laser Phys. Lett.* **14**, 045202 (2017)
22. N. Metwally, S.S. Hassan, Estimation of pulsed driven qubit parameters via quantum Fisher information. *Laser Phys. Lett.* **14**, 115204 (2017). (8pp)
23. J.P. Dowling, K.P. Seshadreesan, Quantum optical technologies for metrology, sensing, and imaging. *J. Lightwave Technol.* **33**, 2359 (2015)
24. N. Metwally, Fisher information of accelerated two-qubit systems. *Int. J. Mod. Phys. B* **32**(5), 1850050 (2018)
25. B.R. Frieden, R.A. Gatenby, *Exploratory Data Analysis Using Fisher Information* (Springer, Arizona, 2007)
26. F. Troiani, On the use of classical and quantum Fisher information in molecular magnetism. *Magnetochemistry* **2**, 33 (2016)
27. N. Metwally, M. Abdelaty, Obada, Quantum teleportation via entangled states generated by the Jaynes–Cummings model. *A.-S.F. Chaos Solitons Fractals.* **22**, 529535 (2004)
28. L. Chotorlishvili, Z. Toklikishvili, Chaotic dynamics of coupled two-level atoms in the optical cavity. *Eur. Phys. J. D.* **47**, 433 (2008)
29. M. Ali, A.R.P. Rau, G. Alber, Quantum discord for two-qubit X states. *Phys. Rev. A.* **81**, 042105 (2010)
30. M.M. Cola, M.G.A. Paris, Teleportation of bipartite states using a single entangled pair. *Phys. Lett. A* **337**, 10–16 (2005)
31. G.-F. Zhang, Thermal entanglement and teleportation in a two-qubit Heisenberg chain with Dzyaloshinski–Moriya anisotropic antisymmetric interaction. *Phys. Rev. A* **75**, 034304 (2007)
32. J. Liu, X. Jing, X. Wang, Phase-matching condition for enhancement of phase sensitivity in quantum metrology. *Phys. Rev. A* **88**, 042316 (2013)
33. X. Xiao, Y. Yao, W.J. Zhong, Y.L. Li, Y.M. Xie, Enhancing teleportation of quantum Fisher information by partial measurements. *Phys. Rev. A* **93**, 012307 (2016)